Transition Metal Complexes of the Novel Tridentate Di-2-pyridylmethanamine (dipa)

Paul V. Bernhardt, Peter Comba,* Anne Mahu-Rickenbach, Sandra Stebler, Silvio Steiner, Katalin Várnagy, and Margareta Zehnder

Institut für Anorganische Chemie, Universität Basel, Spitalstrasse 51, 4056 Basel, Switzerland

Received March 26, 1992

The first row transition metal complexes $[M(dipa)_2]^{n+}$ (dipa = di-2-pyridylmethanamine, M = Fe(III), Fe(II), Co(III), Ni(II) and Cu(II)) have been synthesized in generally high yields. Stability constants for the labile Co(II), Ni(II), and Cu(II) complexes have been determined by potentiometric titrations and are as follows ($\log K_1$, $\log K_2$): 7.63 (1), 6.57 (1); 8.55 (1), 8.25 (1); and 8.89 (1), 7.94 (1). A rather large degree of steric strain within the complexes is evident from the X-ray crystal structures of *rac*-$[Fe(dipa)_2](ClO_4)_2 \cdot 2H_2O$ (monoclinic, $P2_1/n$, a = 9.392 (3) Å, b = 16.749 (3) Å, c = 17.131 (14) Å, β = 96.62 (5)°, Z = 4) *rac*-$[Co(dipa)_2](ClO_4)_3$ (orthorhombic, $Pcca$, a = 17.574 (5) Å, b = 8.568 (2) Å, c = 19.159 (3) Å, Z = 4), *meso*-$[Ni(dipa)_2](S_2O_6) \cdot 4H_2O$ (triclinic, $P\bar{1}$, a = 7.903 (3) Å, b = 9.810 (3) Å c = 10.900 (2) Å, α = 113.10 (3)°, β = 106.01 (3)°, γ = 96.93 (4)°, Z = 1), and *meso*-$[Cu(dipa)_2](ClO_4)_2$ (monoclinic, $P2_1/n$, a = 7.964 (3) Å, b = 10.154 (2) Å, c = 16.842 (4) Å, β = 100.12 (4)°, Z = 2). Molecular mechanics calculations indicate that the formation of *rac*-$[Co(dipa)_2]^{3+}$ in preference to the *meso* isomer is dominant, and this is in agreement with experimental results based on NMR spectra of equilibrated solutions. In the case of Cu(II), formation of the *meso* isomer is not selective, and this was confirmed by the successful Cu(II)-directed template condensation of the *rac* isomer with formaldehyde and nitroethane. Calculations also indicate that the *rac* isomer of the Ni(II) complex is more stable than the crystallized *meso* isomer.

Introduction

Facially coordinating triaza ligands have attracted considerable attention in the field of coordination chemistry. The vast array of both mono- and polynuclear complexes of 1,4,7-triazacyclononane (tacn) comprises complexes of a wide variety of transition metal ions, many of which are not traditionally associated with amine ligands.[1] Although not as extensively studied as tacn, the tridentate ligands 1,1,1-tris(aminomethyl)ethane (tame),[2] tri-2-pyridylmethane (tpym),[3] propane-1,2,3-triamine (trap)[4] and *cis,cis*-cyclohexane-1,3,5-triamine (tach)[5] have been similarly employed as facially coordinating ligands. In all of the above cases, except for trap, the 3-fold symmetry of the tridentate ligands precludes geometric isomerism of their bis complexes. It was shown that the bis(propane-1,2,3-triamine)cobalt(III) complexes may exhibit two geometric isomers, i.e. the centrosymmetric *meso* and the dissymmetric *rac* isomer where the primary amines in the 2-positions of trap may be either trans or cis, respectively.[6] Molecular mechanics calculations predicted an almost equal distribution of *meso*- and *rac*-$[Co(trap)_2]^{3+}$ and this was confirmed by experiment.

A logical extension of this work was toward the dipyridyl analog of trap, di-2-pyridylmethanamine (dipa). Mixed amine/pyridine tridentates exhibiting facial coordination are rare, so the present study was undertaken in order to examine the coordination chemistry of this novel tridentate ligand with some of the first-row transition metal ions. Substitution of primary amines (trap) by pyridyl groups (dipa) has far reaching consequences concerning the stability of metal ions in certain oxidation states. It is well known that imine-type aza ligands (polypyridyls, Schiff bases) stabilize complexes in lower oxidation states relative to their purely

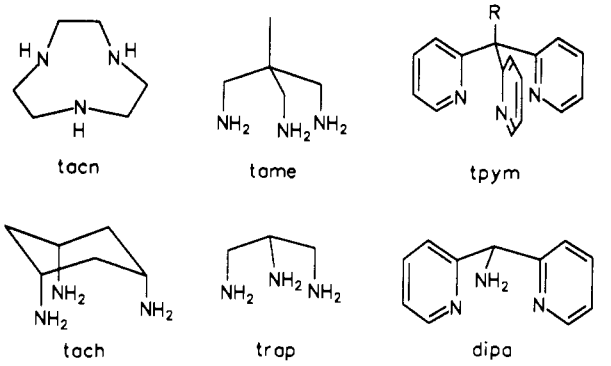

N-donor amine analogs, and this has been attributed, in the main, to the ability of such ligands to delocalize electron density from the metal center via π-back-bonding. The steric bulk of the pyridyl ring relative to a primary amine may also influence the coordination chemistry.

Experimental Section

Syntheses. Di-2-pyridylmethanamine (dipa) was prepared via a literature synthesis.[7,8]

***rac*-Bis(di-2-pyridylmethanamine)iron(III) Triperchlorate, $[Fe(dipa)_2](ClO_4)_3$.** Dropwise addition of a solution of anhydrous $FeCl_3$ (0.44 g, 2.7 mmol) in methanol (100 mL) to a solution of dipa (1.0 g, 5.4 mmol) in methanol (50 mL) afforded a dark red solution from which a yellow precipitate was removed by filtration after 15 min. The precipitate was suspended in 0.5 M $NaClO_4$ (60 mL), stirred at 40 °C for 15 min, and then filtered. The orange product precipitated from the filtrate as a powder within a few hours (0.7 g, 36%). Anal. Calcd for $C_{22}H_{22}Cl_3FeN_6O_{12}$: C, 36.5; H, 3.1; N, 11.6; Cl, 14.7. Found: C, 36.5; H, 3.2; N, 11.7; Cl, 14.6. No d–d electronic maxima were resolved due to the presence of intense charge transfer transitions in the near-ultraviolet and no EPR spectrum was obtainable at 4 K. The complex is spontaneously reduced to the Fe^{II} analog if the filtrate is left to stand for several days.

***rac*-Bis(di-2-pyridylmethanamine)iron(II) Diperchlorate Dihydrate, $[Fe(dipa)_2](ClO_4)_2 \cdot 2H_2O$.** A red solution of $[Fe(dipa)_2]^{2+}$, resulting from

(1) Chaudhuri, P.; Wieghardt, K. *Prog. Inorg. Chem.* **1987**, *35*, 329.
(2) Flückiger, J. R.; Schläpfer, C. W.; Couldwell, C. *Inorg. Chem.* **1980**, *19*, 2493.
(3) Keene, F. R.; Snow, M. R.; Stephenson, P. J.; Tiekink, E. R. T. *Inorg. Chem.* **1988**, *27*, 2040.
(4) Henrick, K.; McPartlin, M.; Munjoma, S.; Owston, P. G.; Peters, R.; Sangokoya, S. A.; Tasker, P. *J. Chem. Soc., Dalton Trans.* **1982**, 225.
(5) Ammeter, J. H.; Bürgi, H.-B.; Gamp, E.; Meyer-Sandrin, V.; Jensen, W. P. *Inorg. Chem.* **1979**, *18*, 733.
(6) Comba, P.; Hambley, T. W.; Zipper, L. *Helv. Chim. Acta* **1988**, *71*, 1875.
(7) Jochims, J. C. *Monatsh. Chem.* **1963**, *94*, 677.
(8) Niemers, E.; Hittmann, R. *Synthesis* **1976**, 593.

0020-1669/92/1331-4194$03.00/0

dropwise addition of a solution of iron(II) chloride tetrahydrate (0.53 g, 2.7 mmol) in methanol (150 mL) to a solution of dipa (1.0 g, 5.4 mmol) in methanol (50 mL) was stirred at room temperature for 30 min. The solution was diluted to 2 L with water and charged on a column (30 cm × 3 cm) of SP Sephadex-C25 ion-exchange resin (Na^+ form). A single red band was eluted with 0.1 M sodium perchlorate solution. The eluate was concentrated on a rotary evaporator and left to crystallize at room temperature (0.16 g, 7%). Several crops were obtained and from the second crop dark red crystals formed that were suitable for X-ray work. Anal. Calcd for $C_{22}H_{22}Cl_2FeN_6O_8 \cdot 2H_2O$: C, 40.0; H, 4.0; N, 12.7; Cl, 10.7. Found: C, 39.4; H, 3.6; N, 12.7; Cl, 11.3. Electronic spectrum (H_2O): λ_{max} 465 nm (ϵ 2600 M^{-1} cm^{-1}), 399 (ϵ 4000). ^{13}C NMR (^1H decoupled, [$^2H_6$]dmso): δ 62.0, 121.0, 122.7, 123.7, 136.4, 136.7, 156.3, 156.8, 163.8, 164.4.

(Di-2-pyridylmethanamine)trinitrocobalt(III), [Co(dipa)$(NO_2)_3$]. The dark brown solution resulting from dropwise addition of an aqueous solution of dipa (3.7 g, 20 mmol, 3 mL of H_2O) to an aqueous solution of $Na_3[Co(NO_2)_6]$ (8.08 g, 20 mmol, 20 mL of H_2O) was heated on a water bath for 30 min. After the mixture was cooled to ambient temperature, the yellow precipitate was removed by filtration and washed with ice–water and methanol and then air-dried (6.8 g, 89%). Anal. Calcd for $C_{11}H_{11}CoN_6O_6 \cdot 0.5H_2O$: C, 33.8; H, 3.1; N, 21.5. Found: C, 33.7; H, 3.1; N, 21.4. ^{13}C NMR (^1H decoupled, ^2H_2O): δ 63.5, 121.0, 123.7, 139.7, 152.1, 158.8.

(Di-2-pyridylmethanamine)trichlorocobalt(III), [Co(dipa)Cl_3]. A solution of [Co(dipa)$(NO_2)_3$] (1.91 g, 5 mmol) in HCl (35 mL, 11 M) was heated for 45 min (90 °C). After the mixture was cooled to room temperature, the resulting dark green product was filtered and washed with ice cold HCl, ethanol, and acetone and air-dried (0.45 g, 26%). Anal. Calcd for $C_{11}H_{11}Cl_3CoN_3$: C, 37.7; H, 3.2; N, 12.0; Cl, 30.3. Found: C, 37.3; H, 3.1; N, 11.9; Cl, 29.8. ^{13}C NMR (^1H decoupled, [$^2H_6$]dmso): δ 66.8, 121.5, 124.4, 140.4, 156.2, 160.9.

(Di-2-pyridylmethanamine)tris(trifluoromethanesulfonato)cobalt(III), [Co(dipa)(trif)$_3$]. [Co(dipa)$(NO_2)_3$] (1.91 g, 5 mmol) was slowly added to neat trifluoromethanesulfonic acid (10 mL), with vigorous stirring in an inert atmosphere (N_2). After being stirred at 90° for 45 min, the purple solution was cooled in an ice bath, and the product was precipitated by addition of dry diethyl ether (50 mL). The hygroscopic product was removed by filtration, washed with ether, and vacuum-dried (2.48 g, 72%). Anal. Calcd for $C_{14}H_{11}F_9CoN_3O_9S_3 \cdot 2CF_3SO_3H$: C, 19.4; H, 1.3; N, 4.2; F, 28.8; S, 16.1. Found: C, 19.9; H, 1.5; N, 4.3; F, 26.0; S, 15.2.

***rac*-Bis(di-2-pyridylmethanamine)cobalt(III) Triperchlorate, [Co(dipa)$_2$](ClO$_4$)$_3$.** Air was bubbled for 12 h through an aqueous solution (5 mL) containing $CoCl_2 \cdot 6H_2O$ (0.95 g, 4 mmol), dipa (1.48 g, 8 mmol), HCl (0.4 g, 11 M), and charcoal (0.5 g). The filtered yellow solution was charged onto a column of Dowex 50 W-X2 cation-exchange resin, which was washed with water before eluting a single yellow band with 3 M HCl. The eluate was evaporated to dryness and washed with ethanol. The yellow powder was recrystallized from dilute sodium perchlorate solution to yield crystals suitable for X-ray work (2.9 g, 70%). Anal. Calcd for $C_{22}H_{22}Cl_3CoN_6O_{12}$: C, 36.3; H, 3.1; N, 11.6; Cl, 14.6. Found: C, 36.4; H, 3.2; N, 11.6; Cl, 14.6. Electronic spectrum (H_2O): λ_{max} 444 nm (ϵ 130 M^{-1} cm^{-1}, $^1T_1 \leftarrow {}^1A_1$). ^{13}C NMR (^1H decoupled, [$^2H_6$]dmso): δ 67.6, 125.3, 125.7, 128.0, 129.4, 144.1, 144.5, 154.1, 154.4, 159.7, 160.5. The same complex could be prepared from reaction of an equimolar ratio of [Co(dipa)(trif)$_3$] and dipa in dry methanol at room temperature. The *rac* isomer was again identified as the sole isomeric species (see Discussion).

***meso*-Bis(di-2-pyridylmethanamine)nickel(II) Dithionate Pentahydrate, [Ni(dipa)$_2$](S$_2$O$_6$)·5H$_2$O.** A solution of $Ni(NO_3)_2 \cdot 6H_2O$ (0.39 g, 1.35 mmol) in methanol (100 mL) was added to a methanolic solution (30 mL) of dipa (0.5 g, 2.5 mmol). After 15 min the purple solution was diluted with water (1 L) and sorbed onto a column of SP Sephadex C25 cation-exchange resin, and a single purple band was eluted with 0.1 M $NaClO_4$. The perchlorate salt crystallized from the eluate upon concentration (0.48 g, 62%). Recrystallization from 0.2 M $Na_2S_2O_6$ (100 mL) afforded crystals of the dithionate salt upon slow evaporation of the filtrate. Anal. Calcd for $C_{22}H_{22}N_6NiO_6S_2 \cdot 5H_2O$: C, 38.9; H, 4.7; N, 12.4; S, 9.4. Found: C, 39.0; H, 4.5; N, 12.5; S, 10.0. Electronic spectrum (H_2O): λ_{max} 860 nm, sh (ϵ 0.8, $^1E_g \leftarrow {}^3A_{2g}$ (O_h)), 787 (ϵ 1.0, $^3T_{2g} \leftarrow {}^3A_{2g}$ (O_h)), 503 (ϵ 1.4, $^3T_{1g} \leftarrow {}^3A_{2g}$ (O_h)).

***meso*-Bis(di-2-pyridylmethanamine)copper(II) Diperchlorate, [Cu(dipa)$_2$](ClO$_4$)$_2$.** To an aqueous solution (100 mL) of $Cu(ClO_4)_2 \cdot 6H_2O$ (0.5 g, 1.3 mmol) was added an aqueous solution (50 mL) of dipa (0.6 g, 3 mmole). Heating (70 °C) of the filtrated solution for 30 min afforded a deep blue solution which was concentrated to half of its volume under reduced pressure. Precipitation was achieved by cooling to 4 °C. The blue powder was collected, washed with ethanol and diethyl ether, and air-dried (0.54 g, 66%). Recrystallization from hot (70 °C) water afforded crystals of X-ray quality. Anal. Calcd for $C_{22}H_{22}Cl_2CuN_6O_8$: C, 41.8; H, 3.5; N, 13.3; Cl, 11.2. Found: C, 41.9; H, 3.6; N, 13.3; Cl, 11.2. Electronic spectrum (H_2O): λ_{max} 616 nm (ϵ 70 M^{-1} cm^{-1}, $^2T_2 \leftarrow {}^2E$). EPR spectrum (DMF:H_2O, 1:2): $g_\parallel$ 2.23, $g_\perp$ 2.08, $A_\parallel$ 188 × 10^{-4} cm^{-1}, $A_\perp$ 23 × 10^{-4}. Excessive heating or standing for more than 3 days in aqueous solution at ambient temperature leads to decomposition of the product.

(4-Methyl-4-nitro-1,1′,7,7′-tetra-2-pyridyl-2,6-diazaheptane)copper(II) Diperchlorate, [Cu(mnpdipa)](ClO$_4$)$_2$. To a solution of $Cu(NO_3)_2 \cdot 3H_2O$ (0.66 g, 2.7 mmol) and dipa (1 g, 5.4 mmol) in methanol (100 mL) were added nitroethane (1 mL, 14 mmol) and triethylamine (1 mL, 7 mmol). A solution of formaldehyde (1 mL, 37%) in 25 mL of methanol was added over a period of ca. 1 h. The mixture was stirred at 40 °C over 3 h and then diluted with water (500 mL) and charged onto a column of SP Sephadex C25 resin. The product was eluted with 0.2 M $NaClO_4$ and precipitated, upon concentration, as a blue powder (0.3 g, 15%). Anal. Calcd for $C_{26}H_{27}Cl_2CuN_7O_{10}$: C, 42.7; H, 3.7; N, 13.4; Cl, 9.7. Found: C, 41.8; H, 4.0; N, 13.3; Cl, 9.5. Electronic spectrum (H_2O): λ_{max} 605 nm (ϵ 110 M^{-1} cm^{-1}) ($^2T_2 \leftarrow {}^2E$). EPR spectrum (DMF:H_2O, 1:2): $g_\parallel$ 2.22, $g_\perp$ 2.09, $A_\parallel$ 187 × 10^{-4} cm^{-1}, $A_\perp$ 21 × 10^{-4}.

Physical Methods. Electronic spectra were recorded on a Cary 2300 spectrophotometer. Infrared spectra (KBr disks) were measured with a Perkin-Elmer FT-IR 1600 instrument. EPR spectra (fluid or frozen solutions, ≈10^{-4} M) were recorded on a Varian E9 spectrometer fitted with a Varian E101 temperature control unit, a Bruker ER035 NMR gaussmeter, and a Marconi Instruments 2440 microwave counter. Proton-decoupled ^{13}C NMR spectra were measured on a Varian GEMINI 300 instrument at 75 MHz with 1,4-dioxane employed as an internal standard. Chemical shifts are cited versus tetramethylsilane. Electrochemical measurements were performed with a Metrohm E612 potentiostat in conjunction with a Metrohm E611 detector. A glassy-carbon working electrode, a Pt-wire counter electrode, and a calomel reference electrode were used in all experiments. For differential pulse polarography, scan rates of 2 mV/s and pulses of 10 mV were adopted. In cyclic voltammetry measurements, the scan rate was 100 mV/s. All compounds were measured as ca. 1 mM solutions which were 0.1 M in $NaClO_4$ and purged with N_2 prior to measurement.

Potentiometric titrations were performed with a Metrohm 665 Dosimat, a Metrohm 605 pH meter, and a thermostated sample compartment (25 °C) with a Metrohm glass electrode. The electrode was calibrated with buffer solutions of pH 4.0 and 7.0, using values of pK_w = 13.848 and an activity coefficient for H^+ of 0.966. An IBM compatible computer employing the program AUTOTIT was used to control the titration and data were analyzed with the program TITFIT,[9] which uses the following definition of complex formation constants:

$$\beta_{MLH} = [M_mL_lH_h]/[M]^m[L]^l a_H{}^h$$

a_H is the hydrogen ion activity.

The titrations were performed with a 0.5 M NaOH solution in the pH range 2.0–10.0 and at 0.5 M ionic strength (KCl), the ligand and metal ion concentrations spanned the range 1 to 4 mM, and metal ion:ligand ratios of 1:1, 1:2, and 1:3 were investigated each in duplicate. For each titration, 50 volume/pH pairs were used for the calculation of the stability constants according to the method prescribed by TITFIT.[9] All chemicals were of analytical reagent quality.

Molecular Mechanics. Force field calculations were performed with the strain energy minimization program MOMEC87,[10] using a force field that has been published elsewhere.[11] Trial coordinates were generated with the graphics program SMILE.[12]

Structure Analyses. The data were collected on an Enraf-Nonius CAD4 diffractometer employing graphite-monochromated Mo Kα radiation and operating in the $\omega/2\Theta$ scan mode ($2 < \Theta < 28$). No corrections for extinction were made. Crystal data are given in Table I. All structures were solved by Patterson techniques using SHELXS-86[13] and refined by

(9) Kaden, T. A.; Zuberbühler, A. *Talanta* **1982**, *29*, 201.
(10) Hambley, T. W. MOMEC-87. A Program for Strain Energy Minimization. University of Sydney, 1987.
(11) Bernhardt, P. V.; Comba, P. *Inorg. Chem.* **1992**, *31*, 2638.
(12) Eufri, D.; Sironi, A. *J. Mol. Graphics* **1989**, *7*, 165.
(13) Sheldrick, G. M. SHELXS-86. A Program for Crystal Structure Solution. University of Göttingen, 1986.

Table I. Crystal Data

	$[Fe(dipa)_2](ClO_4)_2 \cdot 2H_2O$	$[Co(dipa)_2](ClO_4)_3$	$[Ni(dipa)_2](S_2O_6) \cdot 4H_2O$	$[Cu(dipa)_2](ClO_4)_2$
space group	$P2_1/n$ (No. 14)[a]	*Pcca* (No. 54)	$P\bar{1}$ (No. 2)	$P2_1/n$ (No. 14)[a]
a, Å	9.392 (3)	17.574 (5)	7.903 (3)	7.964 (3)
b, Å	16.749 (3)	8.568 (2)	9.810 (3)	10.154 (2)
c, Å	17.131 (14)	19.159 (3)	10.900 (2)	16.842 (4)
α, deg	90.0	90.0	113.10 (3)	90.0
β, deg	96.62 (5)	90.0	106.01 (3)	100.12 (4)
γ, deg	90.0	90.0	96.93 (4)	90.0
V, Å^3	2676.66	2884.85	721.61	1340.76
ρ_{calcd}, g cm^{-3}	1.641	1.675	1.522	1.568
formula	$C_{22}H_{26}Cl_2FeN_6O_{10}$	$C_{22}H_{22}Cl_3CoN_6O_{12}$	$C_{22}H_{30}N_6NiO_{10}S_2$	$C_{22}H_{22}Cl_2CuN_6O_8$
fw	661.23	727.74	661.34	632.90
Z	4	4	1	2
μ, cm^{-1}	8.27	9.42	8.73	10.71
temp, K	293	293	293	293
λ, Å	0.710 69	0.710 69	0.710 69	0.710 69
$R(F_o)$, $R_w(F_o)$[b]	0.046, 0.053	0.058, 0.065	0.059, 0.065	0.061

[a] Variant of $P2_1/c$. [b] $R(F_o) = \sum(||F_o| - |F_c||)/\sum|F_o|$, $R_w(F_o) = \sum(||F_o| - |F_c||)w^{1/2}/\sum|F_o|w^{1/2}$.

difference Fourier methods with CRYSTALS.[14] Scattering factors not given in CRYSTALS were taken from the literature,[15] and plots were produced with ORTEP.[16] All non-hydrogen atoms were refined anisotropically, except for minor contributors to perchlorate anion disorder (O atoms). The H atoms for the Co(III), Ni(II), and Cu(II) structures were fixed at estimated positions whereas H atoms within the Fe(II) structure were refined. The atomic positional parameters for all structures are given in Tables II–V, and selected interatomic distances and angles are combined in Tables VI and VII respectively. Complete listings of bond lengths and angles, H atom coordinates, thermal parameters, observed and calculated structure factor amplitudes, and full crystal data are available as supplementary material.

Results

Syntheses. All $[M(dipa)_2]^{n+}$ complexes were prepared via relatively straightforward and high-yielding routes. The steric requirements and symmetry of the ligand dictate that only two geometric isomers are possible, that is the facial *meso* (C_{2h}) and the *rac* (C_2) isomers. The lower symmetry of the *rac* isomer results in the two pyridyl groups within the same ligand being inequivalent, and indeed this was found in the ^{13}C NMR spectra of $[Co(dipa)_2]^{3+}$ and $[Fe(dipa)_2]^{2+}$ where each pyridyl resonance was split into a doublet.[17] Species possessing a mirror plane symmetry element, e.g. dipa, $[Co(dipa)(NO_2)_3]$, and $[Co(dipa)Cl_3]$, exhibit six resonances in the ^{13}C NMR spectrum, as a result of both pyridyl moieties being equivalent. A similar spectrum would be anticipated for a *meso*-$[M(dipa)_2]^{n+}$ species.

Due to the presence of paramagnetic metal centers, NMR could not be utilized for assignment of the solution structures of the Fe(III), Ni(II), and Cu(II) complexes and solid-state characterization was the only option available. The *meso* isomer was defined in the Cu(II) and Ni(II) complexes from an X-ray crystal structure analysis (see below). That, in solution, there is some *rac* isomer of $[Cu(dipa)_2]^{2+}$ in equilibrium with the *meso* isomer was confirmed by a successful bridging of the two primary amines via a metal-directed condensation with nitroethane and formaldehyde to form $[Cu(mnpdipa)]^{2+}$. The resulting sexidentate ligand mnpdipa is structurally similar to ligands used to mimic type III blue copper proteins.[18] Successful coupling of the two dipa ligands was indicated by the elemental analysis and the IR absorptions of the nitro group (ν_{as}, $\nu_{sym}(NO_2)$ = 1554, 1360 cm^{-1}).

Table II. Atomic Positional Parameters for $[Fe(dipa)_2](ClO_4)_2 \cdot 2H_2O$

atom	x/a	y/b	z/c
Fe(1)	0.21557 (5)	0.03849 (3)	0.23952 (3)
N(1)	0.0614 (3)	0.0052 (2)	0.1620 (2)
N(2)	0.0950 (4)	0.1376 (2)	0.2383 (2)
N(3)	0.2972 (3)	0.0999 (2)	0.1582 (2)
N(4)	0.3470 (3)	−0.0514 (2)	0.2347 (2)
N(5)	0.3616 (4)	0.0692 (2)	0.3279 (2)
N(6)	0.1348 (4)	−0.0148 (2)	0.3266 (2)
C(1)	0.0098 (5)	−0.0682 (3)	0.1459 (3)
C(2)	−0.1085 (6)	−0.0815 (3)	0.0940 (3)
C(3)	−0.1783 (5)	−0.0179 (4)	0.0562 (3)
C(4)	−0.1258 (5)	0.0582 (3)	0.0713 (3)
C(5)	−0.0086 (4)	0.0675 (3)	0.1255 (2)
C(6)	0.0595 (4)	0.1459 (2)	0.1520 (3)
C(7)	0.2035 (4)	0.1519 (2)	0.1218 (2)
C(8)	0.2380 (5)	0.2033 (3)	0.0645 (3)
C(9)	0.3756 (6)	0.2030 (3)	0.0445 (3)
C(10)	0.4730 (5)	0.1511 (3)	0.0828 (3)
C(11)	0.4317 (4)	0.1002 (3)	0.1383 (3)
C(12)	0.3742 (5)	−0.0958 (3)	0.1737 (3)
C(13)	0.4824 (6)	−0.1523 (3)	0.1785 (3)
C(14)	0.5640 (6)	−0.1629 (3)	0.2489 (4)
C(15)	0.5355 (5)	−0.1193 (3)	0.3128 (3)
C(16)	0.4264 (4)	−0.0639 (3)	0.3036 (2)
C(17)	0.3833 (5)	−0.0099 (3)	0.3660 (2)
C(18)	0.2372 (5)	−0.0339 (3)	0.3851 (2)
C(19)	0.2062 (6)	−0.0706 (3)	0.4536 (3)
C(20)	0.0671 (7)	−0.0875 (3)	0.4615 (3)
C(21)	−0.0383 (6)	−0.0683 (3)	0.4023 (3)
C(22)	−0.0018 (5)	−0.0321 (3)	0.3356 (3)
Cl(1)	0.3019 (1)	0.21479 (7)	0.48198 (7)
O(1)	0.1908 (6)	0.1829 (4)	0.4334 (3)
O(2)	0.2599 (6)	0.2355 (3)	0.5554 (3)
O(3)	0.4043 (7)	0.1531 (4)	0.4962 (3)
O(4)	0.3665 (8)	0.2776 (4)	0.4500 (4)
Cl(2)	0.7287 (1)	0.15018 (9)	0.31623 (8)
O(5)	0.6800 (5)	0.0785 (3)	0.3454 (4)
O(6)	0.8562 (5)	0.1733 (4)	0.3594 (3)
O(7)	0.7683 (6)	0.1329 (5)	0.2406 (3)
O(8)	0.6250 (6)	0.2061 (4)	0.3086 (5)
O(9)	0.8355 (6)	0.2398 (3)	0.7717 (4)

Neither NMR nor crystallographic data were obtainable for $[Fe(dipa)_2](ClO_4)_3$. Nevertheless, strong evidence was obtained that the *rac* isomer had been formed. The infrared spectra of $[Fe(dipa)_2](ClO_4)_3$ and *rac*-$[Fe(dipa)_2](ClO_4)_2$ were virtually indistinguishable. Moreover, the spectra of $[Fe(dipa)_2](ClO_4)_3$ and *meso*-$[Ni(dipa)_2](ClO_4)_2$[19] displayed some significant reversals of intensity in the region 1500–1450 cm^{-1} which is the

(14) Watkin, D. J. *CRYSTALS*; University of Oxford: Oxford, U.K., 1989.
(15) Cromer, D. T.; Waber, J. C. *International Tables for X-ray Crystallography*; Kynoch Press: Birmingham, U.K., 1974; Vol. 4.
(16) Johnson, C. K. *ORTEP, A Thermal Ellipsoid Plotting Program*; Oak Ridge National Laboratories: Oak Ridge, TN, 1965.
(17) The spectrum of *rac*-$[Fe(dipa)_2]^{2+}$ displayed only 10 resonances, as the result of an accidental degeneracy of one pair of pyridyl C atoms.
(18) Karlin, K. D.; Hayes, J. C.; Zubieta, J. *Copper Coordination Chemistry: Biochemical and Inorganic Perspectives*; Karlin, K., Zubieta, J., Eds.; Adenine Press: New York, 1983; p 457.
(19) The *meso* isomer of $[Ni(dipa)_2](ClO_4)_2$ was identified by an X-ray crystal structure, where the complex was found to be isostructural with the Cu(II) analog. However, the quality of data in the structure of *meso*-$[Ni(dipa)_2](S_2O_6) \cdot 4H_2O$ was superior and thus the perchlorate structure is not reported.

Table III. Atomic Positional Parameters for $[Co(dipa)_2](ClO_4)_3$

atom	x/a	y/b	z/c
Co(1)	0.0000	0.23552 (9)	0.2500
N(1)	0.0816 (2)	0.2288 (5)	0.3171 (2)
C(1)	0.1560 (3)	0.2462 (7)	0.3064 (3)
C(2)	0.2079 (3)	0.231 (1)	0.3606 (4)
C(3)	0.1823 (4)	0.1985 (9)	0.4264 (4)
C(4)	0.1047 (4)	0.1805 (8)	0.4382 (3)
C(5)	0.0562 (3)	0.1940 (7)	0.3822 (3)
C(6)	−0.0296 (3)	0.1730 (7)	0.3825 (3)
N(2)	−0.0453 (3)	0.0880 (5)	0.3156 (2)
C(7)	−0.0664 (3)	0.3292 (7)	0.3720 (3)
C(8)	−0.1089 (4)	0.4140 (9)	0.4194 (3)
C(9)	−0.1395 (4)	0.5544 (8)	0.3981 (3)
C(10)	−0.1272 (4)	0.6075 (7)	0.3331 (4)
C(11)	−0.0835 (3)	0.5207 (6)	0.2868 (3)
N(3)	−0.0540 (2)	0.3846 (5)	0.3071 (2)
Cl(1)	0.06994 (7)	0.7616 (2)	0.39105 (7)
O(1)	0.0013 (3)	0.8211 (6)	0.4208 (3)
O(2)	0.0675 (3)	0.5967 (5)	0.3857 (2)
O(3)	0.0796 (3)	0.8296 (6)	0.3236 (2)
O(4)	0.1320 (3)	0.8060 (7)	0.4351 (3)
Cl(2)	0.2500	0.0000	0.1262 (1)
O(5)	0.3103 (5)	0.058 (1)	0.0900 (4)
O(6)	0.2168 (7)	0.112 (2)	0.1693 (7)

Table IV. Atomic Positional Parameters for $[Ni(dipa)_2](S_2O_6)\cdot 4H_2O$

atom	x/a	y/b	z/c
Ni(1)	0.5000	0.5000	0.5000
N(1)	0.2337 (5)	0.5167 (4)	0.4191 (4)
N(2)	0.4249 (6)	0.3567 (5)	0.2799 (4)
N(3)	0.3864 (5)	0.2842 (5)	0.4823 (4)
C(1)	0.1557 (6)	0.6319 (5)	0.4688 (5)
C(2)	−0.0232 (7)	0.6217 (7)	0.3973 (6)
C(3)	−0.1255 (7)	0.4914 (8)	0.2732 (7)
C(4)	−0.0463 (7)	0.3715 (6)	0.2215 (6)
C(5)	0.1348 (6)	0.3917 (5)	0.2979 (5)
C(6)	0.2400 (7)	0.2714 (6)	0.2531 (5)
C(7)	0.2629 (7)	0.1967 (5)	0.3524 (6)
C(8)	0.1657 (9)	0.0496 (7)	0.3130 (7)
C(9)	0.198 (1)	−0.0056 (8)	0.4123 (9)
C(10)	0.326 (1)	0.0832 (8)	0.5470 (9)
C(11)	0.4183 (7)	0.2282 (7)	0.5789 (6)
S(1)	0.5645 (2)	−0.0343 (1)	0.0791 (1)
O(1)	0.5925 (7)	0.0931 (5)	0.2133 (4)
O(2)	0.7331 (8)	−0.0580 (8)	0.0585 (6)
O(3)	0.442 (1)	−0.1734 (7)	0.0453 (7)
O(4)	0.193 (2)	0.658 (1)	0.121 (1)
O(5)	0.828 (2)	0.666 (2)	0.049 (2)
O(6)	0.404 (3)	0.459 (3)	0.040 (3)

characteristic region for C=C and C=N vibrations of the pyridyl rings. More concrete evidence was obtained from electrochemical measurements. It was found that both $[Fe(dipa)_2]^{3+}$ and *rac*-$[Fe(dipa)_2]^{2+}$ exhibited identical, reversible $Fe^{III/II}$ redox couples ($E_{1/2}$ = +0.71 V vs SHE), implying that the two complexes are each other's complement within the redox couple. With typically inert low-spin Fe(III) and Fe(II) complexes, one can rule out a *meso–rac* isomerization accompanying electron transfer.

In an effort to obtain the *meso* isomer of $[Co(dipa)_2]^{3+}$ from a nonequilibrated solution, the reactive $[Co(dipa)(trif)_3]$ complex was synthesized. The trifluoromethanesulfonato (triflato) ligand has been found to be an excellent leaving group from a variety of traditionally inert transition metal ions,[20] and thus offers the possibility of isolating kinetically favored, but less stable, isomers. It is notable that $[Co(dipa)(trif)_3]$ may be made by reaction of the trichloro or the trinitro precursor. We believe that the latter method provides a new route toward triflato complexes and offers many advantages over the more traditional chloro substitution. The nitro complexes are much more inert to substitution in aqueous solution than their chloro analogs; thus, the preparation of the precursor to the triflato complex is facilitated. In addition, the

(20) Lawrance, G. A. *Chem. Rev.* **1986**, *86*, 17.

Table V. Atomic Positional Parameters for $[Cu(dipa)_2](ClO_4)_2$

atom	x/a	y/b	z/c
Cu(1)	0.0000	0.0000	0.0000
N(1)	0.2026 (6)	−0.0487 (5)	−0.0513 (3)
C(1)	0.3186 (9)	−0.1440 (7)	−0.0293 (5)
C(2)	0.4471 (9)	−0.1651 (8)	−0.0715 (6)
C(3)	0.461 (1)	−0.087 (1)	−0.1374 (6)
C(4)	0.3424 (9)	0.0099 (9)	−0.1607 (4)
C(5)	0.2151 (7)	0.0269 (6)	−0.1151 (4)
C(6)	0.0761 (8)	0.1290 (7)	−0.1340 (4)
N(2)	−0.0800 (6)	0.0679 (6)	−0.1131 (3)
C(7)	0.1239 (8)	0.2484 (6)	−0.0811 (4)
C(8)	0.193 (1)	0.3587 (8)	−0.1102 (6)
C(9)	0.241 (1)	0.4606 (8)	−0.0570 (8)
C(10)	0.217 (1)	0.4489 (9)	0.0209 (7)
C(11)	0.1455 (9)	0.3375 (8)	0.0440 (5)
N(3)	0.1003 (7)	0.2364 (6)	−0.0052 (3)
Cl(1)	0.0976 (3)	0.1745 (2)	0.2775 (1)
O(1)	0.1276 (8)	0.2345 (6)	0.3522 (3)
O(2)	0.040 (1)	0.0427 (6)	0.2906 (5)
O(3)	0.2344 (9)	0.167 (1)	0.2410 (5)
O(4)	−0.0409 (9)	0.2337 (9)	0.2273 (4)

Table VI. Selected Bond Lengths (Å) and Angles (deg)

	Fe^{II}	Co^{III}	Ni^{II}	Cu^{II}
M–N(1)	1.930 (3)	1.926 (4)	2.099 (4)	2.021 (5)
M–N(2)	2.008 (3)	1.953 (5)	2.110 (4)	2.020 (5)
M–N(3)	1.958 (3)	1.931 (4)	2.109 (4)	2.536 (6)
M–N(4)	1.955 (3)			
M–N(5)	1.990 (3)			
M–N(6)	1.964 (3)			
N(1)–M–N(2)	81.6 (1)	81.7 (2)	78.0 (2)	79.8 (2)
N(1)–M–N(3)	89.2 (1)	90.5 (2)	88.2 (1)	86.4 (2)
N(2)–M–N(3)	79.9 (1)	82.1 (2)	77.8 (2)	72.1 (2)
N(4)–M–N(5)	81.3 (1)			
N(4)–M–N(6)	89.1 (1)			
N(5)–M–N(6)	80.3 (1)			
C(6)–N(2)–M	98.6 (2)	99.2 (3)	98.7 (3)	103.1 (4)
C(17)–N(5)–M	98.7 (2)			
C(5)–N(1)–M	112.5 (3)	112.0 (3)	111.2 (3)	112.4 (4)
C(7)–N(3)–M	112.5 (3)	111.6 (4)	110.4 (3)	102.6 (4)
C(16)–N(4)–M	111.9 (3)			
C(18)–N(6)–M	111.6 (3)			

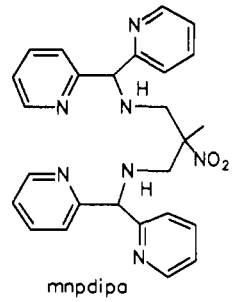

mnpdipa

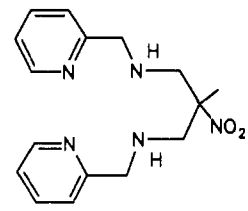

mnppic

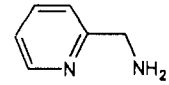

pic

$[Co(NO_2)_6]^{3-}$ complex is a readily available starting material to a wide range of nitro–Co(III) complexes in contrast to the $[CoCl_6]^{3-}$ analog.

Stability Constant Determinations. Potentiometric titration of the protonated dipa ligand yielded pK_a values of $pK_2 \sim 1.7$ and $pK_3 = 7.32$ (1). The first deprotonation step occured at a pH too low to allow its determination, and the second is also rather uncertain since it lies close to the low pH limit of the experiment. The pK_a values of the structurally related 2-(aminomethyl)pyridine (pic, pK_1 = 2.05 and pK_2 = 8.70)[21] are

(21) Huber, P. R.; Griesser, R.; Sigel, H. *Inorg. Chem.* **1971**, *10*, 945.

Table VII. Comparative M–N Bond Lengths (Å) [and $M^{III/II}$ Redox Couples (V vs SHE)]

	$(dipa)_2$	$(bpy)_3$[a]	$(terpy)_2$[b]	sar[c]
Fe(II)	2.00, 1.95 [+0.71]	1.96[d] [+0.97][g]	1.89, 1.99[e] [+0.95][h]	2.20 (high spin)[f] [+0.07][i]
Co(III)	1.95, 1.93 [+0.07]	1.91[j] [+0.31][m]	1.89, 1.92[k]	1.97[l] [−0.44][n]
Ni(II)	2.11, 2.10	2.08[o]	2.06, 2.10[p]	2.13[f]
Cu(II)	2.02, 2.54 [−0.23]	2.03, 2.34[q]	1.98, 2.18[r]	2.11, 2.28[f]

[a] bpy = 2,2′-bipyridyl. [b] terpy = 2,2′:6′,2″-terpyridine. [c] sar = 3,6,10,13,16,19-hexaazabicyclo[6.6.6]eicosane. [d] Garcia Posse, M. E.; Juri, M. A.; Aymonio, P. J.; Diro, O. E.; Negra, H. A.; Castellano, E. E. *Inorg. Chem.* **1984**, *23*, 948. [e] Baker, A. T.; Goodwin, H. A. *Aust. J. Chem.* **1985**, *38*, 207. [f] Comba, P.; Sargeson, A. M.; Engelhardt, L. M.; Harrowfield, J. M.; White, A. H.; Snow, M. R. *Inorg. Chem.* **1985**, *24*, 2325. [g] Smith, G. F.; Richter, F. P. *Ind. Eng. Chem., Anal. Ed.* **1944**, *16*, 580. [h] Dwyer, F. P.; Gyarfas, E. C. *J. Am. Chem. Soc.* **1954**, *76*, 6321. [i] Martin, L. L.; Ph.D. Thesis, Australian National University, 1986. [j] Ohasi, Y.; Yanagi, K.; Mitsuhashi, Y.; Nagata, K.; Sasada, Y.; Kobyashi, H. *J. Am. Chem. Soc.* **1979**, *101*, 4739. [k] Figgis, B. N.; Kucharski, E. S.; White, A. H. *Aust. J. Chem.* **1983**, *36*, 1563. [l] Balahura, A. J.; Ferguson, G.; Ruhl, B. L.; Wilkins, R. G. *Inorg. Chem.* **1983**, *22*, 3990. [m] Weaver, M. J.; Nettles, S. M. *Inorg. Chem.* **1980**, *19*, 1641. [n] Bond, A. M.; Lawrance, G. A.; Lay, P. A.; Sargeson, A. M. *Inorg. Chem.* **1983**, *22*, 2010. [o] Wada, A.; Katayama, C.; Tanaka, J. *Acta Crystallogr., Sect. B.* **1976**, *32*, 3194. [p] Arriortua, M. I.; Rojo, T.; Amigo, J. M.; Germain, G.; Declercq, J. P. *Bull. Soc. Chim. Belg.* **1982**, *92*, 337. [q] Anderson, O. *J. Chem. Soc., Dalton Trans.* **1972**, 2597. [r] Arriortua, M. I.; Rojo, T.; Amigo, J. M.; Germain, G.; Declercq, J. P. *Acta Crystallogr. Sect B* **1982**, *38*, 1323.

comparable, although somewhat higher. The presence of the extra pyridyl substituent on dipa evidently lowers the basicity of both the primary amine and the neighboring pyridyl moiety as a result of its electron-withdrawing effect. The formation constants of dipa with Co(II) (log K_1 = 7.63 (1), log K_2 = 6.57 (1)), Ni(II) (log K_1 = 8.55 (1), log K_2 = 8.25 (1)) and Cu(II) (log K_1 = 8.89 (1), log K_2 = 7.94 (1)) were determined. The constants determined for the Cu(II) complex are slightly smaller than those of $[Cu(pic)_2]^{2+}$ (log K_1 = 9.72, log K_2 = 7.75).[21] In all cases, the values for log (K_1/K_2) were consistent with an initial formation of $[M(dipa)]^{2+}$ then of $[M(dipa)_2]^{2+}$.

Crystal Structures. $[Fe(dipa)_2](ClO_4)_2 \cdot 2H_2O$. The structure consists of the complex cation, two perchlorate anions and two water molecules all on general positions. The *rac* isomer of $[Fe(dipa)_2]^{2+}$ is apparent in Figure 1a, where the two primary amines occupy cis positions. The Fe–N(pyridine) bonds are shorter than the Fe–N (amine) bond lengths (Table VI), but both sets are typical of low-spin iron(II) complexes containing similar donor sets (Table VII). Considerable strain is apparent within the five-membered chelate rings. In particular, the C–N(amine)–Fe angles are all less than 100° and the C–N(pyridyl)–Fe angles are approximately 112°. These are general trends throughout the $[M(dipa)_2]^{n+}$ structures.

$[Co(dipa)_2](ClO_4)_3$. In this structure, the complex cation and one perchlorate anion were situated on a 2-fold axis whereas the remaining pair of symmetry-related anions lay on general sites. The *rac* isomer is again defined in Figure 1b. Although the Co–N bond lengths are somewhat shorter than those found in the Fe(II) structure, the trends are the same, i.e. shorter Co–N(pyridine) than Co–N(amine) bonds. The bond angles exhibited by the complex are quite similar to those found in the Fe(II) complex as a consequence of the comparable size of the two low-spin metal ions.

$[Ni(dipa)_2](S_2O_6) \cdot 4H_2O$. The complex cation was, like the Cu(II) analog, located on a crystallographic center of symmetry and the *meso* isomer was found to be present (Figure 1c). In this case, the Ni–N(pyridine) and Ni–N(amine) bond lengths are not significantly different. The dithionate anion is displaced well away from the complex cation and makes no hydrogen bonding with the primary amine hydrogens. Such interactions have been shown to occur between dithionate anions and pairs of cis-disposed amines;[22] however, in the present case, this failed to promote crystallization of the *rac* isomer of the complex.

$[Cu(dipa)_2](ClO_4)_2$. The complex cation was located on a center of symmetry, with the perchlorate anions on general sites. This immediately indicated that the *meso* isomer had been crystallized, and a view of the complex is given in Figure 1d. The structure offers a rather rare example of a $Cu^{II}N_6$ species. An elongation along one N(pyridyl)–Cu–N(pyridyl) axis (Cu–N = 2.536 Å) relative to the four remaining Cu–N distances (~2.02 Å) is apparent. That is, the complex does not possess a mirror plane but instead a rotation–reflection symmetry element. Such distortions along one L–Cu–L axis are typical of Cu(II) complexes and are a result of a Jahn–Teller distortion operative on the d^9 metal ion in an octahedral ligand field.

Molecular Mechanics. The bis(dipa) complexes presented herein possess no conformational freedom, and therefore molecular mechanics calculations need only consider two species, the *meso* and *rac* isomers. The *rac*/*meso* isomer distributions may be determined by minimization of the strain energy (E_T) of each isomer and then insertion of the strain energies[23] into eq 1.

$$[meso]/[rac] = 0.5 \exp\{(E_T(rac) - E_T(meso))/RT\} \quad (1)$$

The calculations were performed on the $[M(dipa)_2]^{n+}$ (M = Co(III), Fe(III), and Ni(II)) complexes, as these systems are within the scope of available force fields. The results are presented in Table VIII. The only system that could be genuinely tested with experiment was $[Co(dipa)_2]^{3+}$. In this case, the predicted selective formation of the *rac* isomer was verified experimentally. Neither thermodynamically equilibrated solutions nor direct substitution on $[Co(dipa)(trif)_3]$ produced any *meso* isomer. With the Fe(III) and Ni(II) complexes, thermodynamically equilibrated solutions might contain isomer mixtures; however, analysis of the distribution of isomers in solution was not possible. It is notable that the observed *meso*-$[Ni(dipa)_2]^{2+}$ is predicted to be less stable than its *rac* isomer, but the former is evidently less soluble.

Spectroscopy and Electrochemistry. The solution electronic spectra of the bis(dipa) complexes were dominated by intense charge transfer transitions in the near ultraviolet, so only low-energy visible maxima were discernible (see Experimental Section). Nevertheless, the spectra of the Co(III) and Ni(II) complexes defined dipa as a ligand high in the spectrochemical series, slightly higher than 2,2′-bipyridyl.

The solution electronic spectra of $[Cu(dipa)_2]^{2+}$ and $[Cu(mnpdipa)]^{2+}$ are quite similar, and indeed not significantly different from the $[Cu(pic)_2]^{2+}$ and $[Cu(mnppic)]^{2+}$ analogs, which share the same respective structures in the absence of one pair of trans pyridyl groups.[24] The EPR spectra of $[Cu(dipa)_2]^{2+}$ and $[Cu(mnpdipa)]^{2+}$ were typical of tetragonally distorted Cu(II) complexes and again quite similar to the spectra exhibited by $[Cu(pic)_2]^{2+}$ and $[Cu(mnppic)]^{2+}$.

Electrochemistry of the $[M(dipa)_2]^{n+}$ complexes identified quasireversible and reversible $M^{III/II}$ couples for the Co(III) and Fe(III) complexes respectively (Table VII). Irreversible $Cu^{II/I}$ waves were identified for $[Cu(dipa)_2]^{2+}$ and $[Cu(mnpdipa)]^{2+}$, with the latter complex also exhibiting an irreversible nitro group reduction at $E_{1/2}$ = −0.45 V vs SHE. No waves were identified for $[Ni(dipa)_2]^{2+}$ within the potential limits set by neutral aqueous solution.

(22) Creaser, I. I.; Geue, R. J.; Harrowfield, J. M.; Herlt, A. J.; Sargeson, A. M.; Snow, M. R.; Springborg, J. *J. Am. Chem. Soc.* **1982**, *104*, 6016.

(23) The assumption is made that the strain energy is equatable with the free energy, which is reasonable when considering chemically similar isomeric systems such as these.[6] The statistical factor of 0.5 accounts for the two enantiomers of the *rac* isomer.

(24) Comba, P.; Hambley, T. W.; Lawrance, G. A. *Helv. Chim. Acta* **1985**, *68*, 2332.

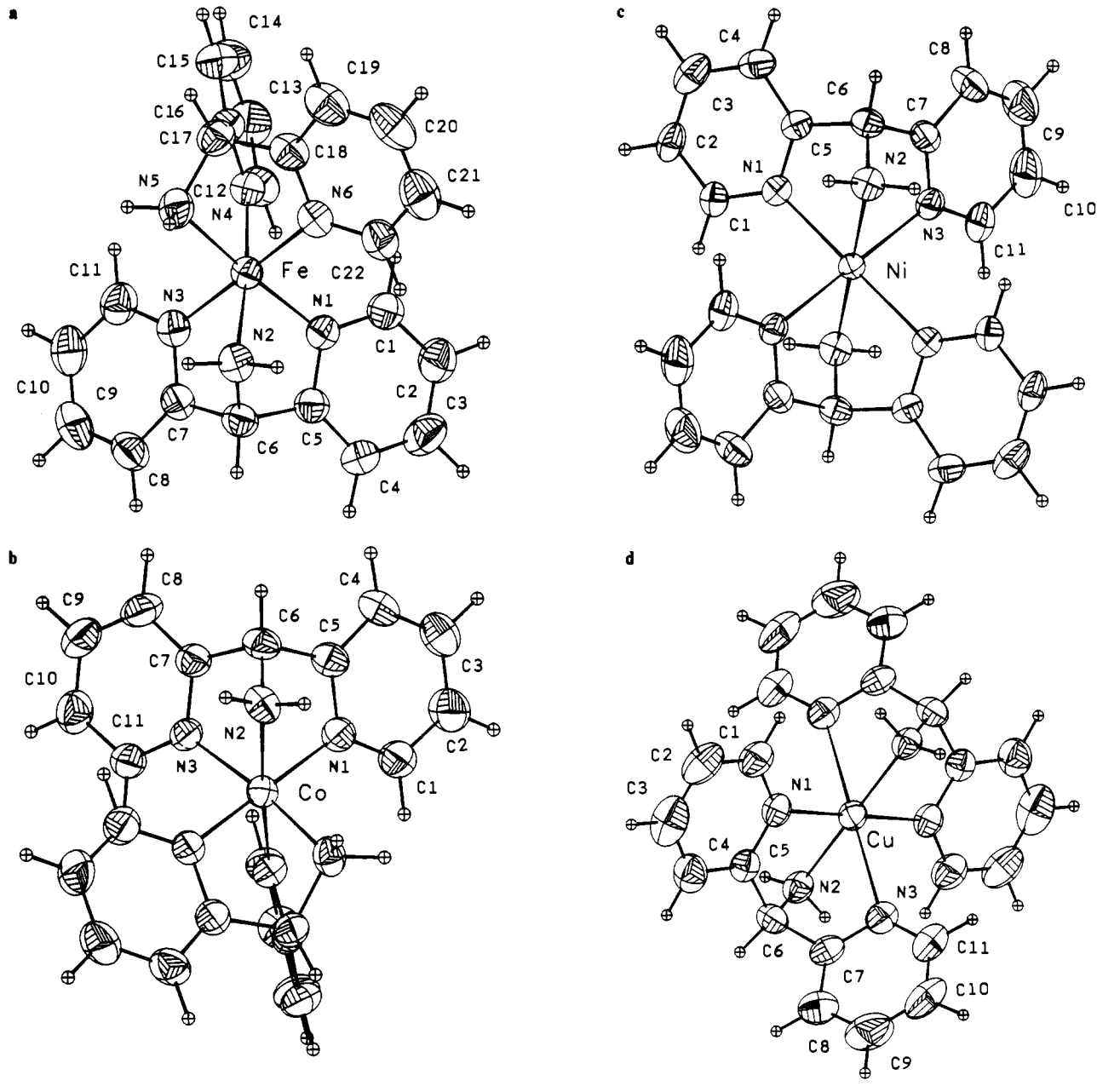

Figure 1. ORTEP plots and atom numbering scheme for the cations: (a) *rac*-$[Fe(dipa)_2]^{2+}$; (b) *rac*-$[Co(dipa)_2]^{3+}$; (c) *meso*-$[Ni(dipa)_2]^{2+}$ and (d) *meso*-$[Cu(dipa)_2]^{2+}$.

Table VIII. Comparison of Experimental and Calculated Structural and Thermodynamic Properties for $[M(dipa)_2]^{n+}$ (M = Fe(III), Co(III), and Ni(II))

compound	M–N(amine), M–N(pyridine) (Å) obsd	M–N(amine), M–N(pyridine) (Å) calcd	% rac/% meso (298 K)
rac-$[Fe(dipa)_2]^{3+}$		2.02, 1.99	87/13
meso-$[Fe(dipa)_2]^{3+}$		2.01, 1.99	
rac-$[Co(dipa)_2]^{3+}$	1.95, 1.93	1.96, 1.93	95/5 (100/0)[a]
meso-$[Co(dipa)_2]^{3+}$		1.96, 1.93	
rac-$[Ni(dipa)_2]^{2+}$		2.12, 2.07	76/24
meso-$[Ni(dipa)_2]^{2+}$	2.11, 2.10	2.13, 2.06	

[a] Experimental value.

Discussion

Although each $[M(dipa)_2]^{n+}$ complex was positively characterized in the solid state, the Co(III) system was the only one where a genuine analysis of the solution equilibrium between the *meso* and *rac* isomers was made experimentally. In the case of the labile Ni(II) and Cu(II) complexes, precipitation of either isomer will disturb the equilibrium, and thus the crystallized complex need not be more stable but merely less soluble than the other isomer. There was also no guarantee that the Fe(II) and Fe(III) systems had come to equilibrium.

Two different methods were employed for the synthesis of $[Co(dipa)_2]^{3+}$. Oxygenation of an aqueous solution of Co^{2+} and stoichiometric amounts of dipa in presence of charcoal produces a thermodynamically equilibrated mixture of isomers.[25] From the reaction mixture, only the *rac* isomer was identified. Attempts to produce the *meso* isomer via the reactive $[Co(dipa)(trif)_3]$ complex, without equilibration, were also unsuccessful. These results are in stark contrast with those obtained from the $[Co(trap)_2]^{3+}$ system where almost equal proportions of *rac* and *meso* isomers were identified from an equilibrated mixture.[6]

A molecular mechanics analysis of the two isomeric forms of $[M(dipa)_2]^{n+}$ was quite revealing in terms of the preference of various metal ions for each isomer. The critical factor determining the distribution of *rac* and *meso* isomers throughout the series of bis(dipa) complexes was the size of the metal ion. Molecular mechanics calculations predict that the *rac* isomers of the Co(III), Fe(III), and Ni(II) complexes are more stable than their

(25) Dwyer, F. P.; Sargeson, A. M. *Nature (London)* **1960**, *187*, 1022.

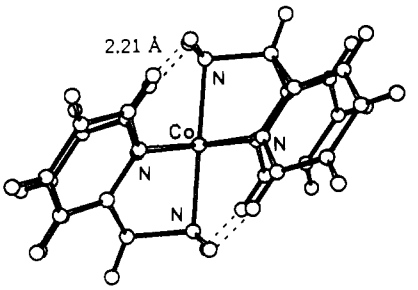

Figure 2. Strain minimized geometry of *meso*-$[Co(dipa)_2]^{3+}$.

corresponding *meso* isomers (Table VIII). Analysis of the individual contributors to the total strain energy for each isomer reveals that the nonbonded interaction terms are the source of their differing stabilities. In particular, an interligand repulsion between the amine hydrogens and the hydrogens ortho to the pyridyl N atoms is the primary cause of the greater nonbonded interaction energies (Figure 2). As the metal ion size increases (Co(III) < Fe(III) < Ni(II)), the H···H replusion is alleviated and the ratio of *meso* to *rac* isomer increases. The *rac* isomers result in a different orientation of the same pairs of interacting H atoms, and indeed no significant H···H repulsion is found.

As expected, the observed $M^{III/II}$ redox couples were found at potentials more positive than those of hexaamine analogs but negative of those for hexaimine relatives (Table VII). The reversibility of the $Fe^{III/II}$ and quasi-reversibility of the $Co^{III/II}$ couples are consistent with chemically stable components of the couple. The $[Cu(dipa)_2]^{2+}$ complex yielded an irreversible $Cu^{II/I}$ couple at a potential somewhat more positive than those for amine analogs. In this case, despite the presence of π-acceptor pyridyl ligands, the monovalent complex is unstable on the voltammetric time scale.

The crystal structures of all $[M(dipa)_2]^{n+}$ complexes revealed that considerable steric strain was a result of coordination of all three N atoms of each ligand. The structures of the Co(III), Fe(II), and Ni(II) complexes revealed essentially octahedral symmetry, with the major deviation being a contraction of the N(amine)–M–N(pyridine) bite angles to ca. 80°. The Jahn–Teller active Cu(II) complex is a rather special case. Although a distortion of the ligand field was anticipated on electronic grounds, the mode of distortion revealed in the crystal structure of $[Cu(dipa)_2](ClO_4)_2$ was interesting in that it did not manifest itself in an elongation of the N(amine)–Cu–N(amine) axis, but rather an elongation of one N(pyridine)–Cu–N(pyridine) axis was found. It is likely that steric strain is an important factor here since elongation of the N(amine)–Cu–N(amine) axis is more demanding on an already strained molecule than an extension along the observed axis.

The Cu(II)-directed coupling of two dipa molecules to form $[Cu(mnpdipa)]^{2+}$ is closely related to the condensation of $[Cu(pic)_2]^{2+}$ with nitroethane and formaldehyde.[24] Indeed, the spectroscopic similarities between $[Cu(mnppic)]^{2+}$ and $[Cu(mnpdipa)]^{2+}$ as well as $[Cu(pic)_2]^{2+}$ and $[Cu(dipa)_2]^{2+}$ indicate that their solution structures are virtually the same; i.e., one pair of *trans* pyridyl groups in $[Cu(dipa)_2]^{2+}$ and $[Cu(mnpdipa)]^{2+}$ are not coordinated in solution. The crystal structure of $[Cu(dipa)_2]^{2+}$ indicated that one pair of *trans* pyridyl groups makes weak bonds with the metal center in the solid state. Potentiometric titration of the free ligand also indicated that the pyridyl N atoms were rather poor nucleophiles so their displacement in aqueous solution is not particularly surprising.

Conclusion

The present study has focused on the bis(dipa) complexes of a variety of first-row transition metal ions in various oxidation states. The presence of the pyridyl groups acts to stabilize a greater variety of complexes than its triamine analog, trap. Molecular mechanics calculations indicated that steric effects play an important role in favoring the *rac* isomer in all cases, and this is also true for $[Ni(dipa)_2]^{2+}$ where the less stable but less soluble isomer was crystallized. Such selectivity was not found in the analogous $[Co(trap)_2]^{3+}$ system.

Acknowledgment. Financial support by the Swiss National Science Foundation (Grant 20-28522.90) is gratefully acknowledged.

Supplementary Material Available: Listings of the H atom coordinates, thermal parameters, bond distances and bond angles, and complete crystal data for $[Fe(dipa)_2](ClO_4)_2 \cdot 2H_2O$, $[Co(dipa)_2](ClO_4)_3$, $[Ni(dipa)_2](S_2O_6) \cdot 4H_2O$, and $[Cu(dipa)_2](ClO_4)_2$ (18 pages). Ordering information is given on any current masthead page.